

# Chapter 7

## Polarization during binary microlensing

### 7.1 Introduction

If electron scattering dominates the opacity at the photosphere of a star, theory predicts that the light should be polarized parallel to the limb up to 11.7% (Chandrasekhar 1960). Rotational ( $R_2$ ) symmetry of the star will cause the photospheric polarization to cancel out. However,  $R_2$  symmetry can be broken by equatorial bulging, by tidal distortion, by eclipse, by exterior illumination, or by amplification due to microlensing. No observations of polarization during microlensing yet exist, but modeling of the observed polarization during microlensing with a single point mass lens shows that the peak polarization is  $\simeq 0.1\%$  for typical lens parameters (Simmons, Newsam, and Willis 1995; Simmons, Willis, and Newsam 1995, hereafter SNW). This is due to differential amplification across the stellar surface. In this paper, we consider polarization during microlensing by a *binary* lens.

There are at least five microlensing events which can be fit with lensing by two masses: MACHO #1, OGLE #6, OGLE #7, DUO #2, and MACHO alert 95-12 (Dominik and Hirshfeld 1994; Mao and Stefano 1995; Udalski et al. 1994; Alard et al. 1995; Pratt et al. 1996). The amplification changes much more rapidly with position during binary lensing than during single lensing, leading to higher observed polarization. The polarization is highest during a caustic crossing, during which the polarization angle flips twice by  $90^\circ$ . Observed po-

larizations can be as high as  $\simeq 1\%$  for an electron scattering atmosphere, which can be measured easily. Absorption opacity can reduce or increase the polarization, depending on the properties of the atmosphere and the wavelength of observation. Scattering from optically thin circumstellar matter can produce additional polarization (Brown, McLean, and Emslie 1978).

Measuring polarization during binary microlensing can be useful in a number of ways: 1) Limb polarization has been difficult to observe in eclipsing binaries due to its low amplitude and due to other polarizing effects such as scattering of light by extended gas and reflection of light by a companion. The first confirmed detection of limb polarization was in Algol (Kemp et al. 1983) at a magnitude of about 0.004%. Polarization during caustic crossing can be higher by an order of magnitude than during occultation, and thus will allow another test of stellar atmosphere theory. 2) The observed polarization could be used to confirm that flux variations are due to microlensing and not due to other sources of variability, such as “bumper stars” (Cook et al. 1995). This is *especially* important for binary microlensing since the variety of possible light curves could mimic other phenomena. 3) If the radius of the star is known, the observed polarization can determine the Einstein radius of the lens. 4) The polarization angle can give the direction of the velocity and the position angle of the binary on the sky. Clearly, a prediction of polarization during binary microlensing is needed to see whether it is measurable and what its signature will be.

Microlensing events that are detected while they are occurring are necessary to obtain polarimetry since accurate polarization cannot be obtained with a survey telescope. Alert systems for the MACHO and OGLE have yielded many alert events so far, which have resulted in well-sampled light curves. This would allow other larger telescopes to take polarimetry after a microlensing event has started.

In section 2 we write down the equations used in the calculation of polarization. In section 3 we calculate the polarization during a fold caustic crossing. In section 4 we describe the calculation of polarization during general binary lensing and show how it can be applied to the above four problems. In section 5 we make some estimates of the possibility of observing polarization during microlensing by a binary. In the last section we summarize and present our conclusions.

## 7.2 Equations

We will define  $r_E$  in the source plane as the Einstein radius of the sum of the binary lens masses projected into the source plane (e.g. Schneider, Ehlers, and Falco 1992):

$$r_E = \sqrt{\frac{4GM D_s D_{ls}}{c^2 D_l}} \quad (7.1)$$

where  $D_s$ ,  $D_l$ , and  $D_{ls}$  are the observer-source, observer-lens, and lens-source distances and  $M$  is sum of the masses of the two lenses. Unless otherwise specified, all distances in the source plane will be expressed in terms of  $r_E$ .

We assume that the limb darkening,  $I(\mu) = I(0)(1 + 2\mu)$ , and polarization,  $P_c(\mu)$ , are given by that of a semi-infinite electron scattering atmosphere (Chandrasekhar 1960). To calculate the polarization of a star at position  $(x_o, y_o)$ , we integrate the unnormalized Stokes quantities and the flux over the star (SNW):

$$\begin{pmatrix} F_Q \\ F_U \\ F \end{pmatrix} = F_o \int_0^{2\pi} \int_0^1 (1 + 2\mu) A_p(x, y) \begin{pmatrix} P_c(\mu) \cos 2\phi \\ P_c(\mu) \sin 2\phi \\ 1 \end{pmatrix} \mu d\mu d\phi, \quad (7.2)$$

where  $\mu$  and  $\phi$  are the spherical coordinates on the surface of the star ( $\phi = 0$  is along the  $x$ -axis and  $\mu=1$  points at the observer),  $x = x_o + r\sqrt{1 - \mu^2} \cos \phi$ ,  $y = y_o + r\sqrt{1 - \mu^2} \sin \phi$ ,  $F_o \equiv I(0)R_\star^2/D_s^2$ ,  $r = R_\star/r_E$ ,  $R_\star$  is the radius of the star, and  $A_p(x, y)$  is the point source amplification in the source plane.  $F_V$  vanishes because scattering is incoherent and thus produces only linear polarization. The normalized Stokes parameters and total amplification are given by:

$$Q(x_o, y_o) = \frac{fF_Q}{F}, \quad U(x_o, y_o) = \frac{fF_U}{F}, \quad \text{and} \quad A_\star(x_o, y_o) = 1 - f + \frac{3fF}{7\pi F_o}, \quad (7.3)$$

where  $A_\star$  is the amplification of the lensed star and  $1 - f$  is the starlight fraction from an unresolved unlensed component. As usual, the polarization is  $P_\star = \sqrt{Q^2 + U^2}$  and the polarization angle is  $\theta_p = 1/2 \tan^{-1} U/Q$  (Chandrasekhar 1960).

The point source amplification,  $A_p(x, y)$ , is analytic for a single mass, which is used to calculate the polarization by SNW. The most striking difference between the amplification of a binary lens and that of a point lens is the existence of fold caustics. For the amplification of a point source close to a fold caustic, there is a 1-D analytic formula derived in (Schneider and Weiß), section 5.1

(1986). This was used to derive an analytic formula for the polarization and amplification near a fold caustic by Schneider and Wagoner (1987). We repeat their calculation in section 3, although we use a slightly more accurate formula for the polarization. For the general 2-D binary lens, the amplification must be found numerically, and this is done in section 4.

### 7.3 Polarization during fold caustic crossing

Near a fold caustic, two images become very bright, merge, and disappear. To describe this, we define coordinates in the source plane such that  $x_c$  is parallel to the caustic and  $y_c$  is perpendicular to the caustic, and corresponding coordinates  $r_x$  and  $r_y$  for the images in the source plane, where  $r_x$  is parallel to the critical curve and  $r_y$  is perpendicular, and  $r_x$  and  $r_y$  are expressed in terms of the Einstein radius in the lens plane. Then, the point source amplification near a fold caustic has a universal scaling given by

$$A_p(y_c) = \begin{cases} g^{1/2}(-y_c)^{-1/2} + A_o & \text{if } y_c \leq 0 \\ A_o & \text{if } y_c > 0 \end{cases} \quad (7.4)$$

for  $|y_c| \ll 1$  (Schneider and Weiß 1986), where  $A_o$  is the amplification of a point source just outside the caustic,

$$g \equiv \left| \frac{\Psi_{xx}}{\Psi_{xxy}} \right| \frac{1}{\sqrt{2(1 - \Psi_{xx})}}, \quad (7.5)$$

and the function  $\Psi(r_x, r_y)$  is the two-dimensional gravitational potential in the lens plane, where subscripts  $x, y$  denote differentiation with respect to the variables  $r_x, r_y$  evaluated where the image crosses the critical curve. Note that for  $y_c < 0$  (“inside”), there are five images, while for  $y_c > 0$  (“outside”) there are three images, for a binary lens with no shear. The first term in equation (7.4) is due to the two images which brighten, merge, and disappear as the source crosses the caustic. The term  $A_o$  refers to the amplification of the other three images which we assume is constant.

Assuming that the caustic is straight and that  $g$  is constant across the star, we can integrate the amplification over the star’s surface to calculate the unnormalized Stokes parameter  $F_Q$  (equation (7.2)) as a function of distance from the caustic. The Stokes parameter  $F_U$  vanishes because the star is symmetric about

the  $y_c$  axis. To make the calculation tractable, we approximate the polarization by

$$P_c(\mu) = p_o \frac{(1 - \mu)(1 - \alpha\mu)}{(1 + 2\mu)}, \quad \alpha = 0.636, \quad p_o = 0.1171. \quad (7.6)$$

Equation (7.6) gives results accurate to  $\sim 10\%$  of the exact polarization for a purely electron scattering atmosphere. Let  $\beta = y_c/r$  be the distance of the caustic from the centre of the star in units of the stellar radius. Then, using equations (7.2) and (7.3) with  $f = 1$ , we perform the  $x_c$  integration since the amplification (7.4) is independent of  $x_c$ . To integrate over the singularity in (7.4), we make a substitution as suggested in (Press et al.), section 4.4 (1992). Then, the polarized flux is  $F_Q = 2I_Q p_o F_o \sqrt{g/r}$  and the total flux is  $F = F_o(2I_F \sqrt{g/r} + 7\pi A_o/3)$ , where  $I_Q$  and  $I_F$  are given by:

$$I_Q(\beta) = \int_l^u \left[ -\frac{4\alpha + 6 + 8\alpha z^2}{3} \sqrt{1 - z^2} + (1 + \alpha)\pi \left( \frac{4z}{\pi} \arccos z + \frac{1}{2} - 2|z| + \frac{3}{2}z^2 \right) \right] dt, \quad (7.7)$$

$$I_F(\beta) = \int_l^u [2\sqrt{1 - z^2} + \pi(1 - z^2)] dt, \quad (7.8)$$

where  $z = \beta + t^2$ , and

$$l = \begin{cases} \sqrt{-1 - \beta} & \text{if } \beta \leq -1 \\ 0 & \text{if } \beta > -1 \end{cases} \quad \text{and} \quad u = \begin{cases} \sqrt{1 - \beta} & \text{if } \beta \leq 1 \\ 0 & \text{if } \beta > 1. \end{cases} \quad (7.9)$$

Then, the polarization is:

$$P_\star(y_c) = \frac{F_Q}{F} = p_o \frac{I_Q(y_c/r)}{I_F(y_c/r) + \frac{7}{6}\pi \sqrt{\frac{r}{g}} A_o}, \quad (7.10)$$

and the amplification is

$$A_\star(y_c) = \frac{3F}{7\pi F_o} = \frac{6I_F(y_c/r) \sqrt{\frac{g}{r}}}{7\pi} + A_o. \quad (7.11)$$

The polarization is defined so that it is positive if the polarization vector is along  $x_c$  and negative if it is along  $y_c$ . These integrals  $I_{Q,F}$  can be expressed in

terms of elliptic integrals (Schneider and Wagoner 1987), although we evaluated the integrals numerically using the routine QROMB (Press et al. 1992). The function  $I_F(\beta)$  has a maximum at  $\beta_{max} = -0.8285$ , and  $I_F(\beta_{max}) = 6.239$ . Thus, the maximum amplification for a given radius for the limb darkening law we are using is

$$A_{*,max}(\beta_{max}r) = 1.70\sqrt{\frac{g}{r}} + A_o. \quad (7.12)$$

In figure 7.1 we illustrate the amplification and percent polarization for a caustic crossing for various stellar radii using the same parameters ( $g = 0.70$ ,  $A_o=1.74$ ) as Schneider and Weiß (1986), their figure 9a. As the star enters the caustic, there is a sharp increase in amplification of the leading edge. Since this edge is amplified much more than the rest of the star, there is a net positive polarization, i.e. the polarization vector is tangential to the limb of the star where the star first crosses the caustic, or along  $x_c$ . When the caustic reaches the centre of the star, around  $y_c = 0$ , the top and bottom edges are amplified, leading to a change in polarization angle by  $90^\circ$  which shows up as a negative polarization, i.e. perpendicular to the caustic, or along  $y_c$ . When the trailing edge enters the caustic, the polarization becomes positive again. The maximum polarization is larger for smaller stars since there is a larger amplification for the part of the star inside the caustic. *This is opposite the dependence for a single lens, in which the polarization is larger for a larger star.* However, this can be confused with absorption opacity, which also changes the polarization magnitude. The zero crossing of the polarization is very sensitive to the source size, so observing the  $90^\circ$  changes in the position angle of polarization should allow an accurate measurement of the stellar radius in terms of the Einstein radius. If the radius of the star is estimated from its spectral type, this yields the Einstein radius of the lens, as SNW pointed out. The radius measured from the polarization light curve can be compared with the radius estimated by frequent monitoring of the amplification during caustic crossing. Once the temperature, stellar type, and radius is known, the effect of absorption can be computed in reducing or increasing the observed polarization amplitude. The dependence of the intrinsic polarization and limb darkening on angle can also change these results if they do not obey the simple electron scattering law. In figure 7.2 is shown the predicted amplification and percent polarization during the first caustic crossing event of OGLE#7 (compared with the results from section 4). In this case,  $g = 0.22$  and  $A_o=1.4$ . Though the caustic crossing takes place over a short period of time (see below), the large polarizations should be easy

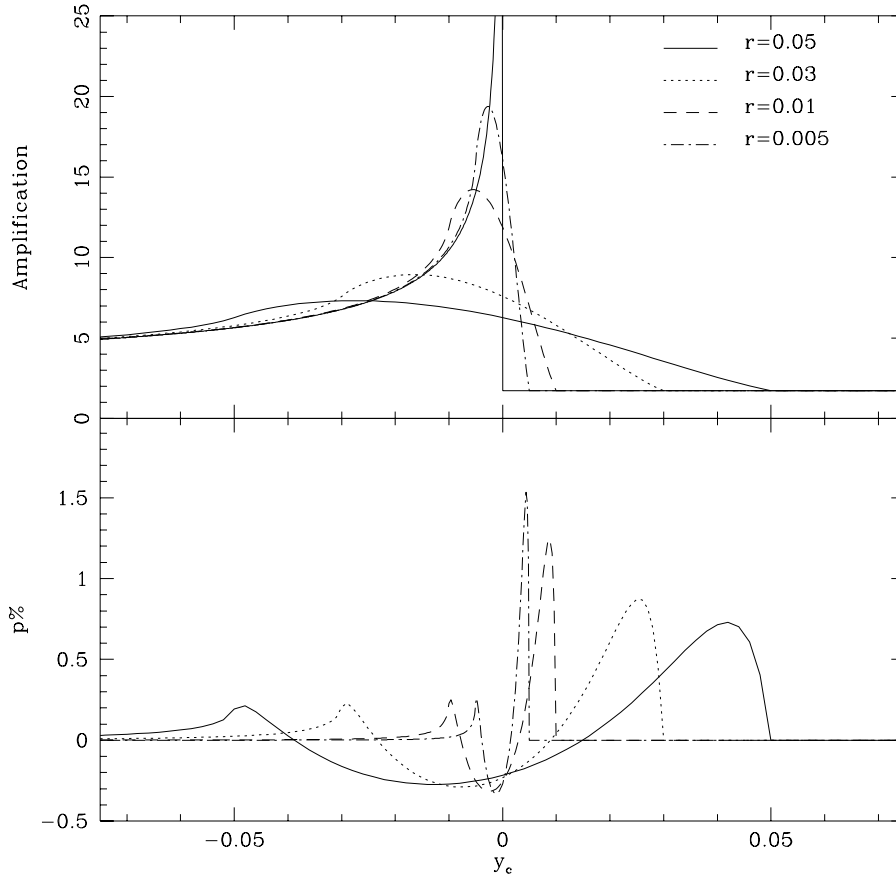


Figure 7.1: Amplification and polarization near a one dimensional caustic. The horizontal axis is the distance of the centre of the star from the caustic,  $y_c$ . The amplification is relative to an unlensed star. The parameters are  $g = 0.7$ ,  $A_o = 1.74$ , which corresponds to the light curve of  $y = 0.3$  for a lens with equal masses (using the coordinates in section 4). The radii,  $r$ , of the the stars are expressed in terms of the Einstein radius of the total mass of the two lenses.

to detect.

The peak polarization for typical microlensing parameters is  $\simeq 1\%$ . Thus, polarization during a caustic crossing could produce a definitive measurement of the limb polarization of a star. Since caustics generally come in well separated pairs, it should be possible to get excellent polarimetry for the second caustic. If an alert event occurs before the source crosses a caustic, it will be possible to see if the polarization signature of a caustic is reproducible.

## 7.4 Polarization during a binary lens event

In this section, we describe a binary lens event by the parameters used in Mao and Stefano (1995), namely the ratio between the masses,  $q = m_2/m_1$ ; the separation of the masses projected onto the lens plane,  $a$ ; the minimum impact parameter of the centre of mass,  $b$ ; the time of closest approach,  $t_b$ ; the time to traverse one Einstein radius,  $t_E$ ; the angle between the velocity direction of the source relative to the lens and the direction from  $m_1$  to  $m_2$ ,  $\theta$ ; and the unlensed fraction of light coming from an unresolved companion star or from the lens itself,  $1 - f$ , which can vary with observation band if the stars are of different spectral type. Hereafter, we will assume the light fraction,  $1 - f$ , from the companion or lens is unpolarized. The coordinate frame  $(x, y)$  has an origin half way between the lens positions projected onto the source plane, and the lenses are taken to lie on the  $x$ -axis (we are using different coordinates than in the previous section).

The point source amplification  $A_p(x, y)$  is computed from the image positions, which are found by solving for the zeros of the fifth order complex polynomial which comes from the complex lensing equation (Witt 1990; Witt and Mao 1995). We used the rootfinding routine LAGUER from Press, Teukolsky, Vetterling, and Flannery (1992). Equations (7.2) are integrated numerically. The root at one point is used as the starting positions for the root finding routine for the next point, since the polynomial coefficients do not change by much except near a caustic.

To test the code, we looked at the polarization for a single lens (i.e.  $a = 0$ ,  $q = 0$ ). The amplification agrees with the analytic formula for a point lens, but the polarization disagrees with that of SNW because we use a more accurate limb darkening law in the calculation of the flux and we use the exact Chandrasekhar formula for the polarization. These effects reduce the polarization in one case

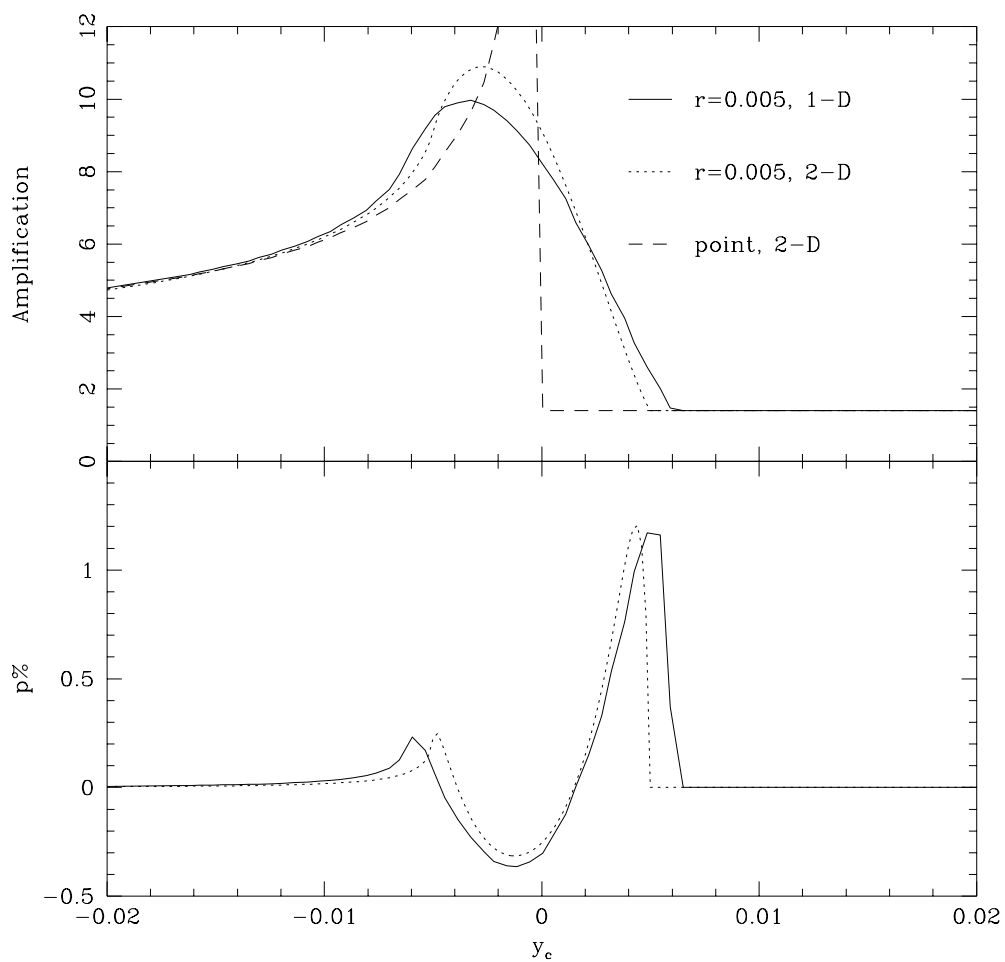


Figure 7.2: Theoretical amplification and percent polarization during the first OGLE #7 caustic crossing. The results of sections 2 (1-D) and section 3 (2-D) are compared.

by a factor of  $\sim 7$  from the SNW result. If we ignore these factors, our code reproduces their results (i.e. their figure 8).

Since the parameter space to explore is rather large, we used the inferred parameters from candidate binary lens events to make predictions of the polarization behavior. Figure 7.2 shows the amplification and percent polarization for OGLE #7 with the binary lens code compared with the results from section 2. The peak polarizations are about the same for both calculations, but the width of the polarization features are different because the caustic is curved and is at an angle to the trajectory of the star so that the caustic crossing time is longer than if the caustic were straight. We used  $r = R_\star/r_E = 0.005$  (based on estimates in Udalski, Szymański, Mao, Stefano, Kałużny, Kubiak, Mateo, and Krzemiński 1994) to calculate the polarization.

The results for OGLE #6 are shown in figure 7.3. The binary lens parameters are  $q = 0.26$ ,  $a = 2.38$ ,  $b = 0.16$ ,  $\theta = 6.2^\circ$ ,  $t_E = 9$  days,  $t_b = 822.7$  days, and  $f = 1$  (Mao and Stefano 1995). This is compared to the polarization expected if the light curve were due to a single lens with parameters  $b = 0.145$ ,  $t_E = 8.4$  days, and  $t_b = 818.9$  days. Thus, polarization is a powerful discriminant between single and binary lenses for a sparsely sampled light curve. However, we can only obtain polarization information during an alert event, so there will also be more frequent and accurate photometry which will already make it easy to distinguish between a double and single microlensing event. The polarization tends to be slightly higher for binary microlensing (without caustic crossing) than for single microlensing, even for the same peak amplification, which will make it somewhat easier to observe. To help visualize the polarization angle, figure 7.4 shows the source plane, with the projected positions of the masses, the caustic pattern, and the polarization angle and amplitude as the source moves across the plane. For a single lens, the polarization angle is always perpendicular to the line between the source and the lens, but for a binary lens, the polarization angle can flip by  $90^\circ$ . This is due to the much more complicated amplification pattern for a binary than a single lens. Measuring a change in polarization consistent with these predictions will lend support to the microlensing interpretation over some other variable phenomenon, since it seems less probable that a variable star would mimic both the amplification *and* the polarization signature of a microlensing event. This is particularly important for the case in which there is achromaticity due to a limb darkening law which changes with wavelength (Gould and Welch 1996) or a companion star of a different color (Griest and Hu 1992) since then only one of the microlensing criteria (e.g. Bennet et al.

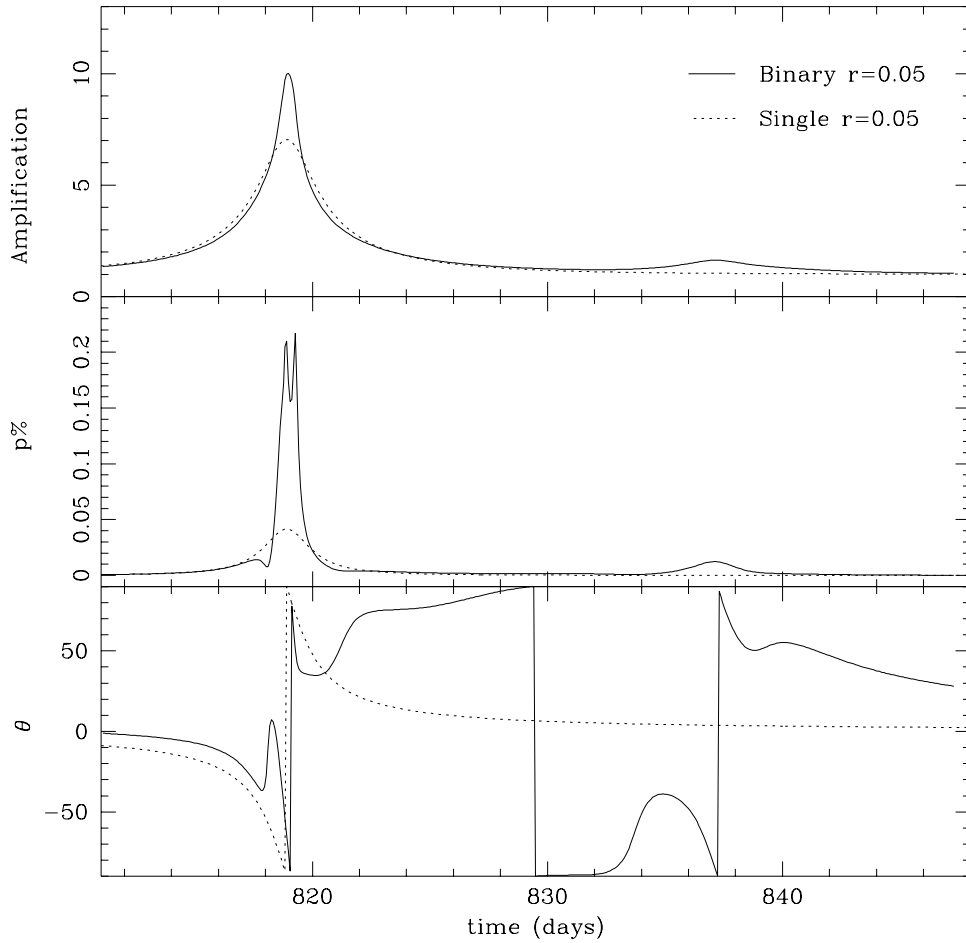


Figure 7.3: Theoretical amplification, percent polarization, and polarization angle ( $\theta_p$ ) during OGLE #6. The fits are taken to be the best single lens fit and the best binary lens fit from Udalski et al. (1994). The reason that the two curves disagree so much near the peak amplification is that the data were sparsely sampled there. The polarization angle is measured relative to the axis between the two lensing masses.

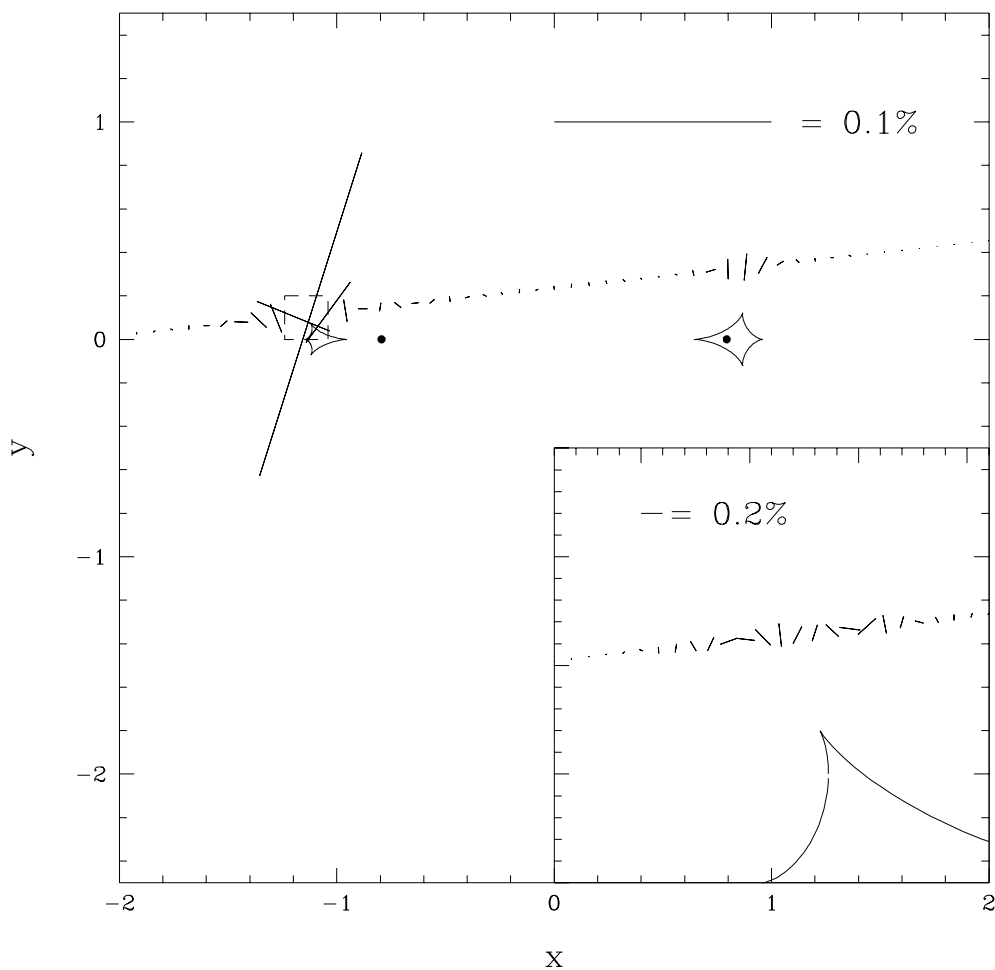


Figure 7.4: Theoretical polarization during OGLE #6, polarization angle and amplitude. The lower right corner is a zoom in of the dashed box in the picture. The polarization scale is also changed in the smaller box to make it more visible. The polarization angle flips twice while passing near the caustic, while for a single lens it would only flip once.

1995) are met if the variability does not repeat. There are a class of variable stars, “bumpers”, discovered by the MACHO group (Cook et al. 1995) which show occasional outbursts which could potentially be fit with a binary lens light curve. They tend to be Be stars, and thus should exhibit limb polarization, which might make it possible to distinguish between bumpers and binary lensing events. Be stars also have winds which could scatter light and cause additional polarization.

We used the parameters inferred from a fit to the microlensing event MACHO #1 with a binary lens (Dominik and Hirshfeld 1994) to make predictions for the polarization behavior of this event. The results are shown in figure 7.5 for various star sizes. The parameters of the fit are  $q = 0.862$ ,  $a = 0.408$ ,  $b = 0.146$ ,  $\theta = 66^\circ$ ,  $t_E = 16.3$  days,  $t_b = 433$  days, and  $f = 1$  (Dominik, private communication). This light curve was originally fit with a single lens light curve, which fit well except for one point at the peak of the amplification (Alcock et al. 1995). Dominik and Hirshfeld (1994) fit the light curve much better with a binary lens model. If this had been an alert event, the light curve would have been well sampled and revealed the binary nature of the lens. As the star size increases, the amplification and polarization angle barely change, but the polarization magnitude increases dramatically. This is because the difference in amplification across a star is larger for larger stars than for smaller, as for a single lens. As was found by SNW, the polarization peak is narrower than the amplification peak. Thus, by varying the radius of the star to fit both the amplification and polarization light curves, one can obtain a limit on the radius of the source. Again, polarization would allow determination of whether the lens is binary or the event is due to some other burst phenomenon.

Figure 7.6 shows the amplification and predicted percent polarization and polarization angle for DUO #2. The lensing parameters are  $q = 0.33$ ,  $a = 1.21$ ,  $b = 0.40$ ,  $\theta = 94.62^\circ$ ,  $t_E = 8.5$  days,  $t_b = 85.4$  days, and  $f = 0.7$  (Alard et al. 1995). The polarization during caustic crossing looks similar to the results from section 2, and the angle flips by  $90^\circ$  twice during caustic crossing. The third change in angle just as the star enters the caustic is due to the difference in direction between the gradient in amplification just outside the caustic and the angle of the caustic where the star first touches. The polarization angle during caustic crossing fixes the angle of the lens on the sky, and since  $\theta$  can be found by fitting the amplification light curve, this fixed the velocity direction on the sky. The third peak is a passage of the star near a cusp. This gives polarizations that are nearly as large as the caustic crossing polarization.

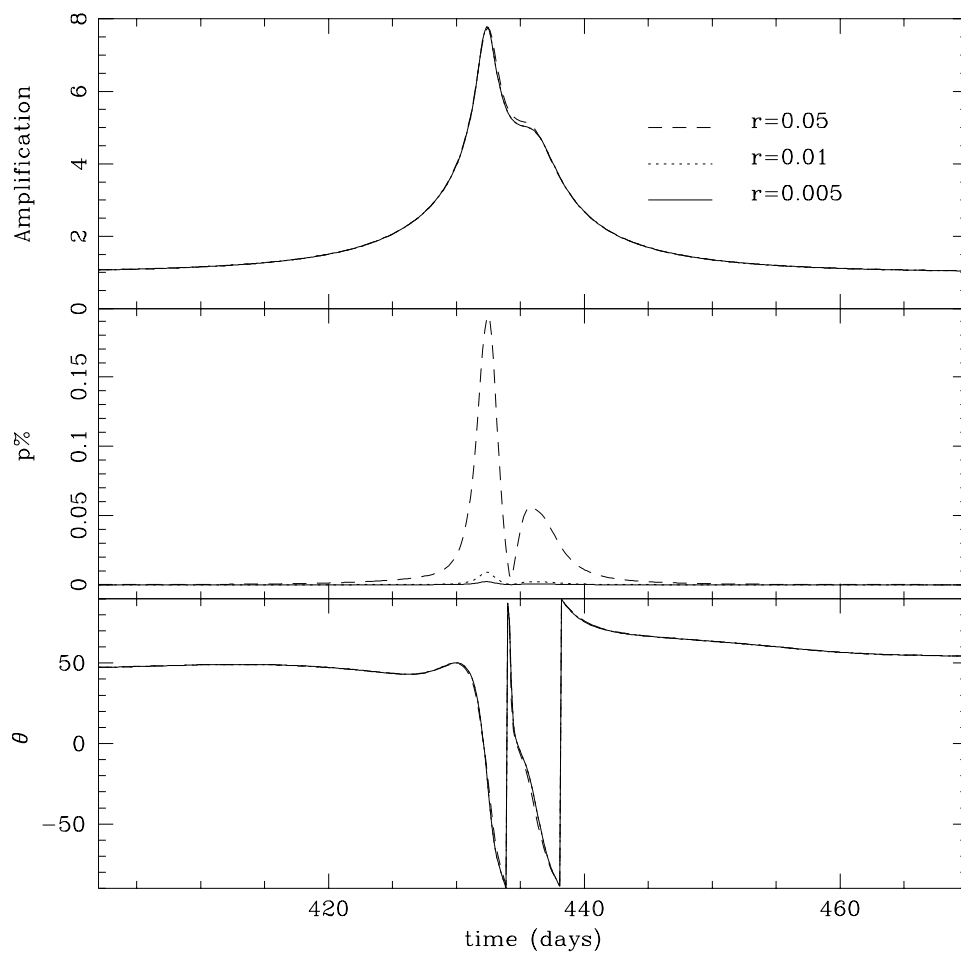


Figure 7.5: Theoretical amplification, percent polarization, and polarization angle during MACHO #1, for stars of various radii,  $r$ .

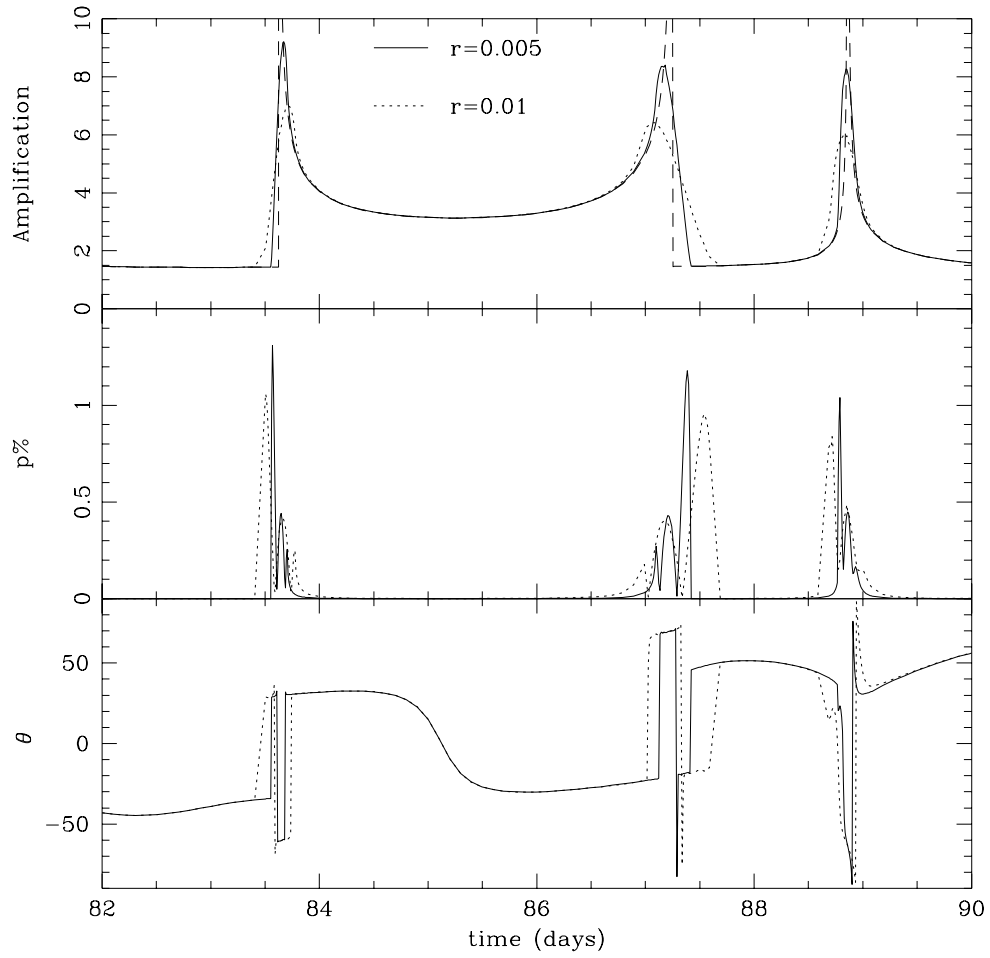


Figure 7.6: Theoretical amplification, percent polarization, and polarization angle during DUO #2.

## 7.5 Observational prospects

From statistical considerations of microlensing towards the galactic bulge, the average mass of microlenses is  $\langle m / M_\odot \rangle \simeq 0.1$  (Han and Gould 1996). If we assume the same average holds for the halo microlensing events, this corresponds to an Einstein radius of

$$r_E = 1 \times 10^{14} \text{cm} (1/\xi - 1)^{1/2} (m/0.1 M_\odot)^{1/2}, \quad (7.13)$$

for  $D_s=50\text{kpc}$  to the Large Magellanic Clouds, where  $\xi = D_l/D_s$ , and  $D_l$  is the distance to the lens. For stars in M31,

$$r_E = 4 \times 10^{13} \text{cm} (D_{ls}/8\text{kpc})^{1/2} (m/0.1 M_\odot)^{1/2}, \quad (7.14)$$

for lenses in the M31 halo at a distance of 8kpc from the source star, or

$$r_E = 10^{14} \text{cm} (D_{ls}/8\text{kpc})^{1/2} (m/0.1 M_\odot)^{1/2}, \quad (7.15)$$

for lenses in our halo, where  $D_{ls} = D_s - D_l$ . Thus, for a large star (e.g. blue giant), the ratio of radius to the Einstein radius of an average lens is  $r \simeq 10 R_\odot / r_E \simeq 0.007 - 0.02$ . Except during caustic crossing, polarization is larger for larger  $r$ , which corresponds to larger  $R_\star$ , smaller  $m$ , and larger  $\xi$ . During caustic crossing, polarization is highest for smaller  $r$ . The caustic crossing has a duration

$$t_\star = \frac{R_\star}{V_t \xi} \simeq 10 \text{ hours } \xi^{-1} \left( \frac{V_t}{200 \text{km/s}} \right)^{-1} \left( \frac{R_\star}{10 R_\odot} \right) \quad (7.16)$$

where  $V_t$  is the transverse velocity of the lens on the sky. If the lens is in the Milky Way, then  $\xi \ll 1$ , making the time scale quite long. This time is long enough to allow polarimetry observations (see below). There are probably more lensing objects at lower masses, and polarization should be somewhat higher, except during caustic crossing, for lensing by small MACHOs since  $r$  is larger. However, timescales for these events are short ( $t_E = r_E / \xi v_\perp \simeq 5$  days, for  $\xi = 0.5$ ,  $m = 0.001 M_\odot$ , and  $v_\perp = 200 \text{ km/s}$ ) which will make it more difficult to have an alert event which is necessary to get polarimetric data.

Stars with high surface temperatures,  $T > 15,000\text{K}$ , are the most likely candidates for observing polarization since electron scattering dominates the opacity (Chandrasekhar 1960; Unsöld 1942). The bulge of the galaxy does not contain any hot stars, but the LMC and M31 do. If 15% of lensing events are

binary (Mao and Paczyński 1991), then at a rate of  $\sim 3$  microlensing events per year, a binary lensing event should be seen once every  $\sim 2$  years by the current MACHO LMC programme. This estimate assumes that MACHOs have a similar number of binaries as observed stars and that there is no amplification bias in observing binary events versus single lens events. Coincidentally, the first LMC event observed may be a binary lens (Dominik and Hirshfeld 1994), so this binary lensing rate estimate may be rather low. Of the binary events, we are mostly interested in the ones which amplify hot stars (O and B). Approximately 5% of the stars in the MACHO LMC sample are O and B stars, so very few of these events are expected. Currently, microlensing events are selected by their symmetry, achromaticity, and other stringent criteria (Alcock et al. 1995), so there are possibly many binary events that are being overlooked. The microlensing rate towards Andromeda is about 15 times higher than towards the LMC (Gould 1994; Crofts 1992) and there are probably a larger fraction of hot stars that can be monitored at the large distance of M31. Thus, there may be a better chance to see polarization towards M31 than the LMC.

The probability of a caustic crossing during binary microlensing is determined by the “width” (Mao and Paczyński 1991), which they calculate to be 0.13 for typical binary star mass ratios. Again, observations indicate that this estimate is low since two of the four candidate binary lens events can be fit by caustic crossing curves. This may be due to poor statistics, or amplification bias (i.e. caustic crossings cause higher amplification which is easier to observe). Thus, the prospects for observing polarization during caustic crossing may be more favorable than the Mao and Paczyński estimate.

Wilson and Liou (1993) fit the Algol eclipse data of Kemp, Henson, Barbour, Kraus, and Collins (1983) with the electron scattering polarization scaled by a constant. They concluded that from  $4000 - 5500\text{\AA}$ , the limb polarization was about 0.02 of the theoretical polarization due to pure electron scattering so that the magnitude of the observed polarization was 0.004%. If we scale our results by a factor of 0.02, then the maximum polarization for the Ogle #7 lightcurve applied to an Algol-like star for  $r = 0.005$  would be 0.04%, or a *factor of 10* higher than for the eclipse polarization of Algol. The disadvantage is that microlensing does not repeat, but it may be a promising method of measuring the limb polarization of stars.

The interstellar polarization towards the Large Magellanic Cloud has been studied extensively (Mathewson and Ford 1970; Schmidt 1970). The polarization tends to be in the range 0.4-1.0% at an angle of  $30 - 60^\circ$  in the V band

(Schmidt 1976). This is due to interstellar dust extinction, and thus can be found by observations after the microlensing event and then subtracted off.

For a B=18 star observed for 100 minutes with a 4 meter telescope (assuming 10% efficiency), the photon shot noise error in polarization is 0.05%. Observations which are photon shot noise limited have been carried out for brighter objects (Frecker and Serkowski 1976; Magalhaes, Benedetti, and Roland 1984; Jain and Srinivasulu 1991; Kemp and Barbour 1981). For polarization errors smaller than 0.2%, the systematic polarization can be the limiting factor (Serkowski 1974). For example, flexure of the mirror, changing of airmass, and atmospheric seeing can affect the accuracy of the polarization measurement. The systematic polarization can be as low as 0.01% if proper precautions are taken, and thus should not preclude this project. Observing such small polarizations in such faint stars is an ambitious project but should be possible with current technology.

## 7.6 Caveats and conclusions

Wavelength dependent absorption is a very important effect: it can reduce or increase the polarization from the pure electron scattering result, it can change the inclination angle dependence of the polarization, and it can flip the polarization angle by  $90^\circ$  (Gnedin and Silant'ev 1978; Gnedin, Dolginov, Potashnik, and Silant'ev 1973; Collins and Buerger 1974). Detailed stellar atmosphere models which include absorption were calculated by Bochkarev, Karitskaya, and Sakhbullin (1985). They present results for a  $T_{eff} = 15,000\text{K}$  LTE atmosphere with bound-free opacity. At wavelengths longer than the Balmer and Lyman edges, the bound free opacity increases as the wavelength increases, so polarization is highest just redward of each edge. From  $912\text{\AA} < \lambda < 2000\text{\AA}$  the polarization exceeds that of an electron scattering atmosphere. Thus, the most promising place to look for polarization is at wavelengths just longward of each edge (although this may be affected by line blanketing by lines near the edge). In U band, the peak polarization for the  $T_{eff} = 15,000\text{K}$  star is about 5% versus 11.7% for a pure scattering atmosphere as assumed in the calculations here, so the results from this paper can be scaled down by  $\sim 0.5$  for observations in U band.

Measuring polarization during a caustic crossing would be a definitive confirmation of the existence of polarization in the limb of hot stars, and would

test the calculations of polarization in plane-parallel scattering atmospheres. If a wavelength dependence of the polarization were seen, this would reveal the role that absorption opacity plays in determining the stellar polarization. In particular, these calculations are used to compute the polarization from accretion disks for cataclysmic variables and active galactic nuclei (Cheng, Shields, Lin, and Pringle 1988; Laor, Netzer, and Piran 1990). The effects on optical polarization of non-LTE atmospheres and line blanketing have not been calculated, but may be large by changing the temperature and ionization structure near the photosphere.

An alert system which triggers on any quiescent star which suddenly shows variations is necessary to look for binary microlensing, which can show a variety of light curves which do not fit the single lensing, color-free light curve. Currently, all stars with  $V < 17.5$  are cut from the MACHO data to remove the highly variable bumper stars from the data set, which will also eliminate most of the hot stars (Alcock et al. 1995). This criterion will have to be ignored for limb polarization during microlensing to be seen.

We have only considered the photospheric polarization. Circumstellar gas around highly evolved stars in the form of disks or winds can also cause polarization (e.g. Haisch and Cassinelli 1976; Bastien 1988), as suggested by SNW. If the gas is optically thin and highly ionized, or if there is dust scattering, the reflected light can be very highly polarized (Brown, McLean, and Emslie 1978). Also, since this gas is extended, there will be a larger difference in amplification across it than across the star, possibly leading to higher total polarization. Thus, polarization should be searched for in other stars besides hot stars, although no predictions yet exist about what could be seen.

If the microlensed star has an unresolved companion that is not lensed and not polarized, then the polarization will be less than for a single star. If the microlensed star has a companion that is polarized, then the polarization could decrease during microlensing if the polarization angles are orthogonal. If the star is asymmetric due to rotation or tidal disruption, it can be polarized without microlensing.

In conclusion, polarization can be a useful diagnostic during binary microlensing. The main drawback is its low amplitude for typical values of the lensing parameters without caustic crossing. During caustic crossing or passage near a cusp, polarization can be as large as  $\sim 1\%$ , while it is  $\sim 0.1\%$  otherwise. The polarization increases with smaller  $r$  during caustic crossing, while it increases with larger  $r$  otherwise. The predicted polarizations are higher for

microlensing by a double lens than by a single lens. The high amplifications that occur during caustic crossing should make it easier to measure polarization. If polarization can be measured then it can be used to distinguish between microlensing variability and variability due to other effects such as bumper stars, it can be used to determine the Einstein radius, and it can be used to determine the position angle of the lens and relative velocity of the lens on the sky. Polarization can be looked for during all binary microlensing alert events since other polarization mechanisms can cause observable polarization, but it should especially be looked for in hot stars where the results of this paper are applicable.

## 7.7 Acknowledgements

I wish to thank Omer Blaes and Robert Antonucci for their general insights and guidance, Todd Hurt for discussing polarimetric observing, and Hans Witt for advice on lens inversion. Thanks to Stuart Marshall, Kem Cook, and Chris Stubbs for discussions about the MACHO data. Thanks to Martin Dominik for carefully reading the manuscript, suggesting changes, and giving the best-fit parameters for MACHO #1. Thanks to the referee, John Simmons, for his detailed comments and correspondence which greatly improved the presentation of this paper. This work was partially supported by California Space Institute grant CS-16-93.